# Order-disorder phase transition and stress-induced diffusion in Au-Cu

John Hennig,* Daniele Mari, and Robert Schaller
*Group of Mechanical Spectroscopy, Institute of Physics of the Condensed Matter, École Polytechnique Fédérale de Lausanne, Station 3, 1015 Lausanne, Switzerland*†

(Received 3 February 2009; published 24 April 2009)

Isothermal mechanical spectroscopy by means of a forced torsion pendulum (measuring internal friction/mechanical loss) was used to study the interplay of long-range atomic order and stress-induced diffusion (Zener relaxation) in $Au_{57\%}Cu_{43\%}$. Our results show that the relaxation strength of stress-induced diffusion exhibits the typical Curie-Weiss-type behavior in the disordered solid solution and then gradually goes to zero below the critical temperature marking the phase transition to the long-range-ordered AuCu II phase. The breakdown of the relaxation peak reflects the kinetics of the ordering process. The diffusion data were used to establish the transformation time vs temperature (TTT) diagram of the phase transformation.

DOI: 10.1103/PhysRevB.79.144116 PACS number(s): 62.40.+i, 64.70.kd

## I. INTRODUCTION

The gold-copper system is a classic example for atomic ordering in alloys and a popular testing ground for theories predicting alloy phase stability.[1] Forming a random solid solution ($\alpha$ phase) at high temperatures [Fig. 1(a)], it undergoes a solid-solid phase transformation to an ordered phase somewhere below 700 K (depending on composition).[2] In the vicinity of equiatomic AuCu, two ordered structures exist. The phase AuCu I, with a superstructure of tetragonal $L1_0$ symmetry [Fig. 1(b)], is stable at low temperatures. Over a temperature range of a few tens of degrees below the transition from the disordered phase, AuCu II is stable. It differs from AuCu I in that it has (nearly) periodic antiphase boundaries along the $y$ axis (about) every five unit cells.[3]

The kinetics of the ordering processes in Au-Cu have been studied by several authors, using indicators such as the elastic modulus[4] and the electrical resistivity,[5,6] or observing the evolution of the x-ray diffraction patterns[3,7] as a function of annealing time and annealing temperature. The present paper deals with the $\alpha \rightarrow$ AuCu II disorder-order transition in $Au_{57\%}Cu_{43\%}$. This phase transformation is of first order;[3] AuCu II grows in the $\alpha$ phase starting from needle-shaped nuclei.[8]

The lattice structure of most solid solutions is locally distorted ("bond buckling"), a phenomenon that arises from the size mismatch of the alloying elements and which can be observed by means of x-ray absorption fine-structure (XAFS) studies[9] (as opposed to standard x-ray diffraction, which only yields average atom positions). Au-Cu is, again, a prime example, as the size mismatch of Au and Cu is particularly large, creating strong static distortions of the lattice in the $\alpha$ phase.[10]

These lattice distortions in Au-Cu also give rise to a well-known mechanical relaxation: stress-induced diffusion (or stress-induced directional ordering). First described by Clarence Zener in 1947,[11] this *anelastic* phenomenon (reversible, but not instantaneous) is commonly referred to as the Zener relaxation. Under an external stress perturbing the equilibrium as measured by XAFS, the system will rearrange bonds along preferential directions dictated by the stress tensor in order to minimize the total elastic strain energy. The return to equilibrium is driven by short-range diffusion—much like the process of atomic ordering.

Several theories exist describing stress-induced diffusion either as a reorientation of elastic dipoles formed by solute pairs,[12,13] as directional order of (nearest-neighbor) bonds,[14] as variations in short-range order beyond nearest neighbors,[15] or by a lattice gas model.[16] Experimentally, the primary interest lies in the fact that the Zener relaxation time is of the same order of magnitude as the time between atomic jumps but can be measured at temperatures far below those accessible to radio-tracer diffusion experiments.[17]

Long-range-ordered alloys, which, if the order is perfect, are completely free of static distortions, are not susceptible to stress-induced diffusion. While intuitively clear, only the early theory by LeClaire and Lomer[14] accounts for this detail. Experimentally, it was verified in a number of alloy systems, such as Mg-Cd that orders at compositions close to the intermetallic compound $MgCd_3$.[18] However, experimental methods employed at that time (temperature-dependent internal friction measurements at a fixed frequency) made it difficult to study stress-induced diffusion in conjunction with the order-disorder phase transition and therefore never went beyond establishing the existence or absence of the Zener relaxation for a given alloy. The evolution of the relaxation strength during the transition has never been directly observed. Modern isothermal mechanical spectroscopy, which probes the anelastic response of a specimen as a function of frequency of stress excitation at constant temperature, overcomes this limitation.

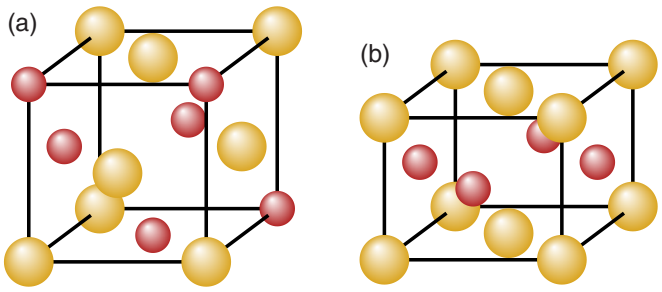


FIG. 1. (Color online) (a) Cubic unit cell of the disordered solid solution of gold (large spheres) and copper atoms (small spheres). (b) Tetragonal unit cell of the AuCu I ordered phase.

 

In the present paper, we will lay out the benefits of isothermal mechanical spectroscopy for the study of order-disorder transitions in alloys via the phenomenon of stress-induced diffusion. While mechanical spectroscopy is a global experimental method and therefore cannot determine alloy superstructures, it offers a quick and reliable way to obtain transition temperatures and ordering kinetics. It may also be seen as a direct observation of the annealing-out of the static lattice distortions evidenced in XAFS. We have chosen an alloy of composition $Au_{57\%}Cu_{43\%}$, which according to the phase diagram[2] undergoes the $\alpha \rightarrow$ AuCu II disorder-order phase transformation at 634 K.

## II. THEORY OF THE ZENER RELAXATION

The theory presented in the following paragraphs mostly follows LeClaire and Lomer.[14] However, in an effort to explain all the qualitative features of our measurements, we have incorporated the approach by Li and Nowick[19] [via Eq. (8)], so as to yield an explicit Curie-Weiss-type [$\propto 1/(T - T_{CW})$] temperature dependence of the relaxation strength of stress-induced diffusion.

Disregarding interactions beyond the nearest-neighbor shell, the crucial parameter governing ordering phenomena in a binary $A$-$B$ alloy is the average bond energy

$$V^p = V^p_{AA} + V^p_{BB} - 2V^p_{AB}. \tag{1}$$

The index $p$ accounts for stress-induced variations in energy among the $\frac{z}{2}$ crystallographic directions along which the $z$ nearest neighbors sit. At zero stress, the bond energies will not depend on $p$, unless the symmetry of the (disordered phase's) lattice is broken by long-range atomic order.

The total internal energy of the crystal can then be expressed in terms of the number of unlike bonds ($N_{AB}$) and like bonds ($N_{AA}$,$N_{BB}$). For fixed atomic fractions $c_A$ and $c_B$, the bond numbers along $p$ direction (throughout the entire crystal, not just one row of atoms) are subject to the conditions

$$N^p_{AA} + \frac{1}{2}N^p_{AB} = Nc_A, \tag{2a}$$

$$N^p_{BB} + \frac{1}{2}N^p_{AB} = Nc_B. \tag{2b}$$

For symmetry reasons, we eliminate $N^p_{AA}$ and $N^p_{BB}$ and choose the relative numbers of unlike bonds,

$$y^p = \frac{\frac{1}{2}N^p_{AB}}{N} \quad [0 \le y^p \le \min(c_A, c_B)], \tag{3}$$

as order parameters.

As the right-hand side of Eq. (2) is constant, one can analogize the dissociation of unlike bonds to a chemical reaction:

$$2A - B \rightleftharpoons A - A + B - B \ \text{(for each } p). \tag{4}$$

The quasichemical approach[20] stipulates that the equilibrium condition be given by the law of mass action applied to this reaction. In terms of $y^p$, it reads as

$$\frac{(c_A - y^p)(c_B - y^p)}{(y^p)^2} = \exp\left(-\frac{V^p}{kT}\right). \tag{5}$$

Taylor expansion around the zero-stress equilibrium values, $y^p_0$ on the left-hand side and $V^p_0$ on the right-hand side, yields

$$\Delta y^p = g(y^p_0)c^2_A c^2_B \frac{\Delta V^p}{kT}, \tag{6}$$

where $\Delta y^p$ and $\Delta V^p$ are the first-order deviations from $y^p_0$ and $V^p_0$, and

$$g(y^p_0) = \frac{(c_A - y^p_0)y^p_0(c_B - y^p_0)}{c^2_A c^2_B(2c_A c_B - y^p_0)}, \tag{7}$$

a function depending on the initial state of order $y^p_0$.

A second equilibrium condition is needed in order to fix either $\Delta y^p$ or $\Delta V^p$. Purely thermodynamics considerations[19] yield that for small variations in the order parameters, $\Delta V^p$ must be of the form

$$\Delta V^p = v_0 \lambda_p \sigma + \sum_q b_{pq} \Delta y^q, \tag{8}$$

where the coupling constants $\lambda_p = (\partial \epsilon / \partial y^p)_{\sigma, y^{q \neq p}}$ will be treated as parameters, $v_0$ designates the volume occupied by a single atom of the unstrained crystal, and the coefficients $b_{pq}$ describe the interaction between order parameters. [The scenario bears resemblance to magnetic materials, where the alignment of permanent magnetic moments in the (disordered) paramagnetic phase under an external magnetic field is amplified by the exchange interaction among the magnetic moments themselves.]

In order to simplify the problem and decouple Eqs. (6) and (8), one disregards off-diagonal terms in $b_{pq}$. Furthermore, since for the cubic lattice all orientations $p$ are crystallographically equivalent at zero stress, $b_{pq}$ is then reduced to a single parameter, $b_{pq} = b\delta_{pq}$.[19]

Once equilibrium is reached, the strain $\epsilon$ has increased with respect to the initial purely elastic strain. This difference, the anelastic strain, can be expressed in terms of the $\Delta y^p$ as

$$\epsilon_{an} = \sum_p \lambda_p \Delta y^p. \tag{9}$$

The same coupling constants $\lambda_p$ appear in this expression due to a reciprocity relation the free-energy differential must adhere to.[19]

Finally, using Eq. (6) into Eq. (8), introducing the Curie-Weiss temperature of stress-induced diffusion,

$$kT_{CW} = bg(y^p_0)c^2_A c^2_B, \tag{10}$$

and resolving for $\Delta V^p$, one obtains

$$\Delta V^p = v_0 \lambda_p \sigma \frac{T}{T - T_{CW}} \tag{11}$$

for the bond energy variation with stress. The singularity $\Delta V^p$ presents at $T_{CW}$ should be interpreted in view of the quasichemical approach [Eq. (5)], which was the starting point of this derivation. $V^p$ approaching (plus or minus) infinity means that $y^p$ takes on one of its extreme values, i.e., the alloy would spontaneously order even for infinitesimal stress values. In practice, however, the transition temperature to long-range atomic order, $T_A$, is higher than $T_{CW}$. To account for this difference, interactions beyond the linear term in Eq. (8) would have to be considered.

The strength of an anelastic relaxation is defined[21] as

$$\Delta = \frac{\epsilon_{an}}{\epsilon_{el}}, \tag{12}$$

where $\epsilon_{el} = \sigma / M_u$ denotes the elastic strain and $M_u$ as the *unrelaxed* elastic (Young's or shear) modulus of the specimen. For the Zener relaxation one then finds [using Eq. (9), then Eqs. (6) and (11) into Eq. (12)]:

$$\Delta = \frac{c_A^2 c_B^2}{k(T - T_{CW})} v_0 M_u \sum_p g(y_0^p) \lambda_p^2. \tag{13}$$

The function $g$ [Eq. (7)], which correlates stress-induced changes to the equilibrium values of $y^p$ and $V^p$, appears in this expression. In a random solid solution, one has $y_0^p = c_A c_B$, and $g(y_0^p)$ takes the value of 1. In a perfectly long-range-ordered structure such as AuCu I [Fig. 1(b)], the zero-stress order parameter $y_0^p$ is either 0 (only like bonds) or $\frac{1}{2}$ (only unlike bonds), depending on $p$, so that $g(y_0^p)$ is zero for all $p$. For the more complicated structure of AuCu II, the result should be virtually the same. While the antiphase boundaries introduce a certain amount of disorder,[8] they are not expected to contribute measurably to stress-induced relaxation since that would involve a collective motion of atoms, not just isolated jumps. Thus, when cooling the solid solution below the temperature of atomic ordering, the Zener relaxation strength should first show an increase of the Curie-Weiss type, $\Delta \propto (T - T_{CW})^{-1}$, and then completely disappear.

## III. EXPERIMENT

Isothermal mechanical spectroscopy readily yields the Zener relaxation strength at any given temperature. In a forced torsion pendulum,[22] the harmonic stress applied to the specimen produces an harmonic strain that, due to stress-induced diffusion, lags behind by an angle $\phi$. The tangent of this phase lag, the mechanical loss tangent, is measured as a function of driving frequency at constant temperature. If stress-induced diffusion is governed by a single relaxation time $\tau$, the frequency spectrum of the mechanical loss tangent takes the form of a Debye peak:[21]

$$\tan \phi(\omega) = \frac{\Delta}{\sqrt{1 + \Delta}} \frac{\omega \tau}{1 + \omega^2 \tau^2}. \tag{14}$$

The peak height, roughly $\Delta/2$ for $\Delta \ll 1$, yields the relaxation strength, while the peak's position, at $\omega = 1/\tau$, reveals the relaxation time.

As diffusion is a thermally activated process, the relaxation time is a function of temperature, following an Arrhenius equation:

$$\tau = \tau_0 \exp\left(\frac{H_{act}}{kT}\right). \tag{15}$$

$H_{act}$ designates the activation enthalpy for atom jumps to neighboring lattice sites that contribute to the relaxation.

Measurements were carried out under a helium atmosphere (7 mbar) on a polycrystalline cylindric specimen (22 mm in length and 2.5 mm in diameter) of $Au_{57\%}Cu_{43\%}$, cast in a graphite crucible after induction melting of 5N-pure gold and copper under vacuum.

## IV. RESULTS AND INTERPRETATION

Figures 2(a) and 2(b) show isothermal frequency spectra of the mechanical loss tangent at selected temperatures around the atomic order-disorder transition. From one scan to the next, the temperature was increased or decreased [Figs. 2(a) and 2(b), respectively] in steps of 5 K.

Initially [i.e., at 610 K in Fig. 2(a)], as a result of a previous thermal treatment, the alloy is ordered. Nevertheless, a small Zener relaxation peak appears in the spectrum. This indicates that the state of atomic order is not perfect. Indeed, due to the nonstoichiometric composition chosen for this experiment, some substitutional disorder must exist: gold atoms occupying sites on the copper sublattice. Only in the perfectly ordered equiatomic AuCu should the peak be absent.

The advantage of using a nonstoichiometric alloy is that one also obtains the Zener relaxation time of stress-induced diffusion in the ordered phase. Results are shown in Fig. 3. Fitting the relaxation times to the Arrhenius Eq. (15) yields a limit relaxation time of $\tau_0^{(o)} = 3.6 \times 10^{-9}$ s and an activation enthalpy $H_{act}^{(o)} = 1.00$ eV.

Due to the variation in the relaxation time, the Zener peak shifts to the right in Fig. 2(a). At the same time the peak height increases. First gradually reflecting the gradual decline of long-range order due to thermal disorder. Then, between 640 and 650 K, much more rapidly, marking the transition from the unstable ordered AuCu II phase to the stable disordered $\alpha$ phase.

The temperature dependence of the Zener relaxation in the disordered phase is observed in Fig. 2(b). The relaxation strength $\Delta$, readily obtained from the peak height, follows, to good approximation, a Curie-Weiss-type law (Fig. 4) in agreement with Eq. (13). Extrapolation of the fit yields a Curie-Weiss temperature of stress-induced diffusion of $T_{CW} = 596 \pm 5$ K.

Just like in the ordered phase, the relaxation time obeys the Arrhenius Eq. (15), as shown in Fig. 3. However, there is

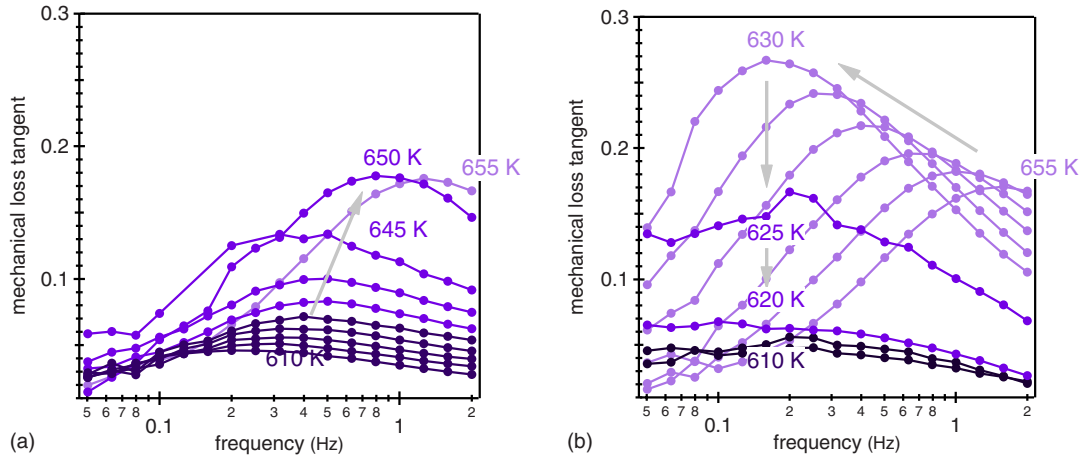


FIG. 2. (Color online) Mechanical loss frequency spectra of $Au_{57\%}Cu_{43\%}$ in isothermal conditions at selected temperatures (steps of 5 K between curves) below and above the order-disorder phase transition. (a) Formation of the Zener relaxation peak (due to stress-induced diffusion) with increasing temperature. (b) Critical evolution of the Zener relaxation peak height with decreasing temperature in the disordered $\alpha$-AuCu phase (light shade), breakdown of the peak during the phase transformation (medium shade) to the ordered AuCu II phase (dark shade).

a noticeable change in slope at the phase transition. For limit relaxation time and activation enthalpy in the disordered phase one finds $\tau_0^{(d)}=1.2\times10^{-20}$ s and $H_{\mathrm{act}}^{(d)}=2.47$ eV, respectively.

Upon cooling below 630 K [again in Fig. 2(b)], the Zener relaxation peak breaks down. This marks the onset of atomic ordering which hinders stress-induced diffusion, except for the contribution due to substitutional disorder in the ordered phase.

Since the disordered $\alpha$ phase is unstable below 630 K, the equilibrium critical temperature of atomic ordering, $T_A$, must be in the vicinity of this value. Section V will explain how to determine $T_A$ with a precision that goes beyond this first approximation.

The hysteresis between heating and cooling observed in Fig. 2 clearly indicates that the phase transformation is of first order: the initial phase first becomes metastable and additional overheating or undercooling is required to render it thermodynamically unstable. After that, the transformation proceeds more rapidly, only limited by the energy barrier of atomic diffusion.

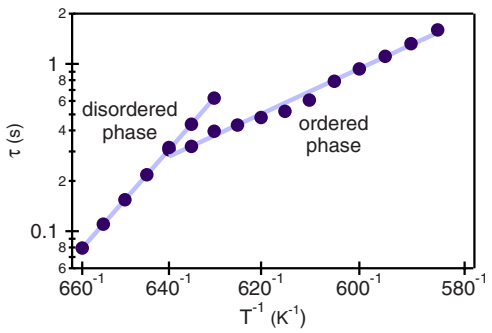


FIG. 3. (Color online) Relaxation time of stress-induced diffusion $\tau$ vs inverse temperature in the disordered and ordered phase along with separate fits to the Arrhenius Eq. (15).

## V. KINETICS OF ATOMIC ORDERING

The gradual breakdown of the Zener peak below the transition temperature can be used to study the kinetics of the ordering process (Fig. 5). To that end, the specimen was first annealed in the disordered state at 680 K for one hour, then quickly cooled below the order-disorder transition temperature $T_A$. After reaching the target temperature, the mechanical loss was monitored over time at a fixed frequency. The evolution of the state of long-range order is reflected in the mechanical loss dropping from an initial value due to stress-induced diffusion in the disordered phase down to the infinite-time value corresponding to maximum order. (For temperatures where ordering is slow, the final value was obtained after establishing order at a lower temperature and subsequent reheating.) We will assume that there is a correspondence between this *relative* relaxation strength and the volume fraction of the disordered phase. The assumption implies that the ordered phase nucleates and grows within the disordered phase.

In Fig. 5, the relative relaxation strength is reported as a function of annealing time. It should be noted that the curves

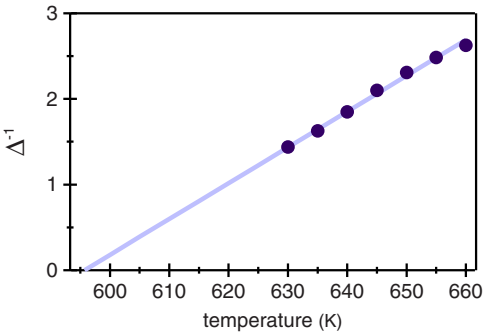


FIG. 4. (Color online) Curie-Weiss-type behavior of the relaxation strength of stress-induced ordering, $\Delta^{-1}\propto T-T_{\mathrm{CW}}$, as obtained from the height of the Zener relaxation peaks in the disordered phase [Fig. 2(b)].

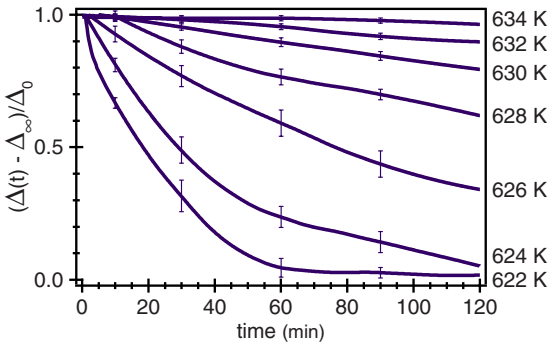


FIG. 5. (Color online) Kinetics of the disorder-order transformation as obtained from (normalized) mechanical loss measurements over time at 1 Hz after quick cooling of the disordered specimen to temperatures below the long-range order transition.

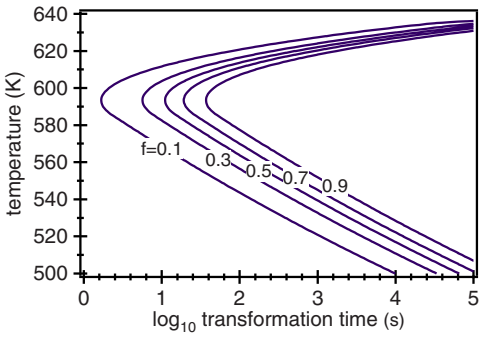


FIG. 6. (Color online) Calculated TTT diagram for the ordering process $\alpha \rightarrow$ AuCu II, showing the volume fraction of ordered phase $f$ as a function of temperature and transformation time.

were smoothed to improve the presentation. The scatter in the data during the phase transformation, indicated by error bars in Fig. 5 and also noticeable in the frequency spectra (Fig. 2), is caused by a shape memory effect that happens to occur in this particular alloy,[23] hampering precision measurements.

In Fig. 5 one can observe that the stronger the undercooling, the faster the ordering process. At 634 K, on the other hand, ordering is so slow that one readily estimates an equilibrium transition temperature of $T_A = 635 \pm 1$ K.

This result can be corroborated by modeling the kinetics of the ordering process. For the present alloy, we base our approach on Šíma's model for equiatomic AuCu,[24] which has proven to agree very well with other experimental data, such as differential calorimetry, x-ray, and resistivity measurements.

It was noted by the former author that the ordering in AuCu does not proceed according to the classical Avrami equation for nucleation and growth processes. Instead, the volume fraction of ordered domains $f$ evolves as a simple exponential: $f \propto 1 - \exp^{-Kt}$. Fits to the data in Fig. 5 confirm this observation for the present $Au_{57\%}Cu_{43\%}$ alloy. Consequently, $f$ must obey a rate equation:

$$\dot{f} = -K^{(d)} f + K^{(o)}(1 - f). \tag{16}$$

For the rate parameters of ordering and disordering we put

$$K^{(o/d)} = \nu_0 \exp\left(-\frac{H_{\text{act}}^{(d/o)}}{kT}\right)\exp\left(-\frac{U^{(o/d)}}{kT}\right), \tag{17}$$

which involves the activation enthalpies $H_{\text{act}}^{(d/o)}$ for diffusion with the disordered/ordered phase as well as the free-energy potential barriers $U^{(o)}$ for ordering and $U^{(d)}$ for disordering. Note that diffusion within the *ordered* phase enters the rate parameter of *disordering* and vice versa.

An advantage of using the Zener relaxation strength as an indicator for long-range order is that it readily provides diffusion data as well. This was pointed out in Sec. I. We use the results for $\tau^{(o)}$ and $\tau^{(d)}$ extracted from Fig. 3 to estimate the respective diffusion activation energy $H_{\text{act}}^{(d/o)}$ in Eq. (17).

Starting from an expression for the Landau free energy of AuCu (derived from an alloy Hamiltonian that takes the electronic properties of Au and Cu into account),[25] Šíma[24] parametrized the potential barriers $U^{(o)}$ and $U^{(d)}$ as a function of the equilibrium transition temperature $T_A$, the discontinuity of the molar entropy $s$, the width of the thermal hysteresis range $\delta$, and some scaling factor $n$ (see the Appendix). Fits to the kinetic data displayed in Fig. 5 then yield: $n = 2470$, $s = 0.31k$, $\delta = 67$ K, and, most importantly, a transition temperature $T_A = 635.3$ K.

Using the full set of parameters, the TTT diagram, Fig. 6, was calculated. It shows the fraction of ordered domains as a function of transformation time and temperature (TTT). Note that the breakdown of the Zener relaxation only yielded kinetic data for temperatures rather close to $T_A$. The typical nose of the TTT diagram as well as the low-temperature part are a result of an extrapolation of the Arrhenius plot of the Zener relaxation times in Fig. 3 to low temperatures, where the high driving force of ordering competes with the slow diffusion.

On a final note, it should be pointed out that the precision of the measurements presented in this paper is due to the stability and calibration of the temperature control (about 1 K). Furthermore, to conduct similar measurements for a given alloy, the frequency range (of the torsion pendulum to be used) has to be chosen such that the Zener relaxation peak appears close to the order-disorder transition temperature.

## VI. CONCLUSIONS

Mechanical spectroscopy measurements have evidenced stress-induced diffusion in the high-temperature disordered phase of $Au_{57\%}Cu_{43\%}$. A Curie-Weiss-type critical behavior of the Zener relaxation strength was observed while cooling down to the order-disorder transition temperature. During the phase transformation the Zener relaxation breaks down, leaving only a residual peak attributed to substitutional disorder in the ordered AuCu II phase. These observations were used to determine the transition temperature as well as ordering kinetics. A TTT diagram for the ordering process was obtained using the activation parameters of the Zener relaxation.

## APPENDIX

According to Šíma,[24] with notation adapted to the present paper, the potential barriers of ordering and disordering in

the temperature interval from $T_A - \frac{3}{4}\delta$ to $T_A + \frac{1}{4}\delta$ read as

$$U^{(o)} = \frac{1}{3} ns\delta[1 - 3l(T) + 2l(T)^{3/2}]$$

and

$$U^{(d)} = \frac{4}{3} ns\delta l(T)^{3/2},$$

where

$$l(T) = \frac{1}{4} + \frac{T_A - T}{\delta}.$$

*john.hennig@epfl.ch
†URL: http://titan.epfl.ch/gsm/

[1] V. Ozoliņš, C. Wolverton, and A. Zunger, Phys. Rev. B **57**, 6427 (1998).
[2] B. Predel, *Au-Cu (Gold-Copper)*, Landolt-Börnstein Group IV Vol. 5a (Springer-Verlag, New York, 1991), Chap. 272, pp. 355–359.
[3] Y. Feutelais, B. Legendre, and M. Guymont, Acta Mater. **47**, 2539 (1999).
[4] S. Siegel, J. Chem. Phys. **8**, 860 (1940).
[5] G. J. Dienes, J. Appl. Phys. **22**, 1020 (1951).
[6] G. C. Kuczynski, R. F. Hochman, and M. Doyama, J. Appl. Phys. **26**, 871 (1955).
[7] J. L. O'Brien and G. C. Kuczynski, Acta Metall. **7**, 803 (1959).
[8] J. Bonneaux and M. Guymont, Intermetallics **7**, 797 (1999).
[9] A. Frenkel, E. A. Stern, A. Voronel, M. Qian, and M. Newville, Phys. Rev. Lett. **71**, 3485 (1993).
[10] A. I. Frenkel, V. S. Machavariani, A. Rubshtein, Y. Rosenberg, A. Voronel, and E. A. Stern, Phys. Rev. B **62**, 9364 (2000).
[11] C. Zener, Phys. Rev. **71**, 34 (1947).
[12] C. Zener, *Elasticity and Anelasticity of Metals* (The University of Chicago Press, Chicago, 1948).
[13] A. S. Nowick and W. R. Heller, Adv. Phys. **12**, 251 (1963).
[14] A. D. LeClaire and W. M. Lomer, Acta Metall. **2**, 731 (1954).
[15] D. O. Welch and A. D. Le Claire, Philos. Mag. **16**, 981 (1967).
[16] H. Wipf and B. Kappesser, J. Phys.: Condens. Matter **8**, 7233 (1996).
[17] A. S. Nowick, Phys. Rev. **88**, 925 (1952).
[18] J. Lulay and G. Wert, Acta Metall. **4**, 627 (1956).
[19] C. Y. Li and A. S. Nowick, Acta Metall. **9**, 49 (1961).
[20] P. Haasen, *Physical Metallurgy*, 2nd ed. (Cambridge University Press, New York, 1986).
[21] A. S. Nowick and B. S. Berry, *Anelastic Relaxation in Crystalline Solids* (Academic Press, New York, 1972).
[22] R. Schaller, G. Fantozzi, and G. Gremaud, *Mechanical Spectroscopy $Q^{-1}$ 2001* (Trans Tech Publications Ltd., Switzerland, 2001).
[23] M. Ohta, T. Shiraishi, R. Ouchida, M. Nakagawa, and S. Matsuya, J. Alloys Compd. **265**, 240 (1998).
[24] V. Šíma, Mater. Sci. Eng., A **324**, 62 (2002).
[25] B. Chakraborty and Z. Xi, Phys. Rev. Lett. **68**, 2039 (1992).